MULTI-PRECISION POLICY ENFORCED TRAINING (MUPPET) : A PRECISION-SWITCHING STRATEGY FOR QUANTISED FIXED-POINT TRAINING OF CNNS

Anonymous authors
Paper under double-blind review

ABSTRACT

Large-scale convolutional neural networks (CNNs) suffer from very long training times, spanning from hours to weeks, limiting the productivity and experimentation of deep learning practitioners. As networks grow in size and complexity, one approach of reducing training time is the use of low-precision data representation and computations during the training stage. However, in doing so the final accuracy suffers due to the problem of vanishing gradients. Existing state-of-the-art methods combat this issue by means of a mixed-precision approach employing two different precision levels, FP32 (32-bit floating-point precision) and FP16/FP8 (16-/8-bit floating-point precision), leveraging the hardware support of recent GPU architectures for FP16 operations to obtaining performance gains.This work pushes the boundary of quantised training by employing a multilevel optimisation approach that utilises multiple precisions including low-precision fixed-point representations. The training strategy, named MuPPET, combines the use of multiple number representation regimes together with a precision-switching mechanism that decides at run time the transition between different precisions. Overall, the proposed strategy tailors the training process to the hardware-level capabilities of the utilised hardware architecture and yields improvements in training time and energy efficiency compared to state-of-the-art approaches. Applying MuPPET on the training of AlexNet, ResNet18 and GoogLeNet on ImageNet (ILSVRC12) and targeting an NVIDIA Turing GPU, the proposed method achieves the same accuracy as the standard full-precision training with an average training-time speedup of 1.28× across the networks.

1 INTRODUCTION

Convolutional neural netwoks (CNNs) have demonstrated unprecedented accuracy in various machine learning tasks, from video understanding (Karpathy et al., 2014; Gan et al., 2015; He et al., 2018) and action recognition (Simonyan & Zisserman, 2014; Ng et al., 2015; Varol et al., 2018) to autonomous drone navigation (Gandhi et al., 2017; Loquercio et al., 2018; Kouris & Bouganis, 2018). To achieve such high levels of accuracy in inherently complex applications, current deep learning methodologies employ the design of large and complex CNN models (He et al., 2016; Szegedy et al., 2017; Huang et al., 2017) trained over large datasets (Deng et al., 2009; Geiger et al., 2013; Lin et al., 2014). Nevertheless, the combination of large models and massive training datasets leads to long training times. This in turn leads to long turn-around times which limits the productivity of deep learning practitioners and prohibits wider experimentation with different model configurations. For instance, automatic tuning and search of neural architectures (Cai et al., 2018; Zhong et al., 2018) is a rapidly advancing area where accelerated training enables improving the produced networks.

To counteract these long turn-around times, substantial research effort has been invested in hyperparameter tuning for training acceleration, with a particular focus on batch size and content. One line of work maximises memory and hardware utilisation by changing the batch size, in order to perform CNN-training-specific prefetching, scheduling and dependency improvement (Chen et al., 2019; Rhu et al., 2016). Other works focus on altering batch size to improve the convergence rate while maintaining high hardware utilisation (Devarakonda et al., 2017) and demonstrating up to 6.25× training acceleration. Alternatively, works such as (Johnson & Guestrin, 2018; Katharopoulos &

Fleuret, 2018; Peng et al., 2019; Loshchilov & Hutter, 2016) reconstruct the minibatches according to the predicted impact of each data element to improve the rate of training convergence, resulting in up to 1.2× overall acceleration.

A number of studies have focused on the use of reduced-precision training schemes. Reduced-precision arithmetic involves the utilisation of data formats that have lower wordlengths than the conventional 32-bit single-precision floating-point (FP32) representation and is an approach for co-optimising processing speed, memory footprint and communication overhead. Existing literature can be categorised into works that use reduced precision to accelerate only the training stage while targeting an FP32 model, and those that target networks with quantised weights. Amongst those that target FP32 networks, one line of work involves utilising different quantisation strategies such as dynamic quantisation (Courbariaux et al., 2015) and stochastic rounding (Gupta et al., 2015) as a means to combat the accuracy loss from quantisation. Nevertheless, the effectiveness of the proposed schemes has been demonstrated on small-scale datasets such as CIFAR-10 and MNIST, and on a limited set of networks. Furthermore, the range of quantisation levels that has been explored varies greatly, with a number of works attacking the problem from an algorithmic level and focusing on mild quantisation levels such as half-precision floating-point (FP16) (Micikevicius et al., 2018), while others focus on lower precisions such as 8-bit floating-point (FP8) (Wang et al., 2018). Finally, quantisation has also been used as a means of reducing the memory and communication overhead in distributed training setups (De Sa et al., 2015; 2017; Alistarh et al., 2017).

At the same time, the characteristics of modern CNN workloads and the trend towards precision-quantised models have led to an emergence of specialised hardware processors, featuring support for low-precision arithmethic at the hardware level. Spanning from custom designs such Google's TPUs (Jouppi et al., 2017) and Microsoft's FPGA-based Brainwave system (Fowers et al., 2018) to commodity platforms such as NVIDIA's Turing GPUs, existing processing platforms include hardware support for reduced precision including 16-bit half-precision floating-point (FP16), and 8-bit (INT8) and 4-bit (INT4) fixed-point data types, thus providing increased parallelism for lower bitwidths. Although these platforms have been mainly designed to target the inference stage of already-trained networks, the reduced-precision hardware offers significant opportunities for accelerating the time-consuming training stage. In this respect, there is an emerging need to provide training algorithms that can leverage these existing hardware optimisations and provide higher training speed.

This work focuses on tackling the field of reduced-precision training from an algorithmic level. Independently of the number of quantisation levels chosen, or how extreme the quantisation is, this work proposes a metric that estimates the amount of information each new training step obtains for a given quantisation level. This approach enables the design of a policy that can decide *at run time* the most appropriate quantisation level for the training process and, due to its agnostic nature, it is orthogonal and complementary to existing low-precision training techniques.

2 Background and Related Work

The state-of-the-art method in training in reduced precision is mixed-precision training (Micikevicius et al., 2018). The authors propose to employ low-precision FP16 computations in the training stage of high-precision CNNs that would perform inference in FP32. Along the training phase, the algorithm maintains a high-precision FP32 copy of the weights of the network, known as a *master copy*. At each minibatch, the inputs and weights are quantised to FP16 with all computations of the forward and backward pass performed in FP16, yielding memory footprint and runtime savings. Under this scheme, each stochastic gradient descent (SGD) update step entails accumulating FP16 gradients into the FP32 master copy of the weights, with this process performed iteratively throughout the training of the network. Micikevicius et al. (2018) evaluate their scheme over a set of state-of-the-art models on ImageNet, and show that mixed-precision training with FP16 computations achieves comparable accuracy to standard FP32 training.

Wang et al. (2018) also presented a method to train an FP32 model using 8-bit floating-point (FP8). The authors propose a hand-crafted FP8 data type, together with a chunk-based computation technique, and employ strategies such as stochastic rounding to alleviate the accuracy loss due to training at reduced precision. For AlexNet, ResNet18 and ResNet50 on ImageNet, Wang et al. (2018) demonstrates comparable accuracy to FP32 training while performing computations in FP8.

Additionally the works presented in (Zhou et al., 2016; Chen et al., 2017) approach the problem of reduced-precision training employing fixed-point computations. FxpNet (Chen et al., 2017) was

only evaludated on CIFAR-10, failing to demonstrate performance on more complex datasets such as ImageNet. DoReFa-net (Zhou et al., 2016) tested on ImageNet but only ran on AlexNet missing out on state-of-the-art networks such as GoogLeNet and ResNet.

All related works focus on accelerating training an FP32 model through reduced-precision computations. At the hardware level, 8-bit fixed-point multiplication uses 18.5× less energy and 27.5× less area with up to 4× lower multiplication times than FP32 (Sze et al., 2017). Consequently, this work attempts to push the boundaries of reduced-precision training by moving to reduced-precision fixed-point computations while updating an FP32 model.

Preliminary tests on training AlexNet and ResNet20 on CIFAR-100 using 8-bit fixed-point computations to update an FP32 model demonstrated that training solely in 8-bit fixed-point results in a significant degradation of validation accuracy compared to full FP32 training (Table 1). This work aims to counteract this degradation by progressively increasing the precision of computations throughout training in an online manner determined by the proposed metric inspired by gradient diveristy (Yin et al., 2018). Additionally by operating in an online fashion, MuPPET tailors the training process to best suit the particular network-dataset pair at each stage of the training process.

Gradient diversity was introduced by Yin et al. (2018) as a metric of measuring the dissimilarity between sets of gradients that correspond to different minibatches. The gradient diversity of a set of gradients is defined as

$$\Delta_{\mathcal{S}}(\mathbf{w}) = \frac{\sum_{i=1}^{n} ||\nabla f_i(\mathbf{w})||_2^2}{||\sum_{i=1}^{n} \nabla f_i(\mathbf{w})||_2^2} = \frac{\sum_{i=1}^{n} ||\nabla f_i(\mathbf{w})||_2^2}{\sum_{i=1}^{n} ||\nabla f_i(\mathbf{w})||_2^2 + \sum_{i \neq j} \langle \nabla f_i(\mathbf{w}), \nabla f_j(\mathbf{w}) \rangle} \tag{1}$$

where $\nabla f_i(\mathbf{w})$ represents the gradient of weights $\mathbf{w}$ for minibatch i.

Yin et al. (2018) argue that if the gradients obtained from consecutive minibatches are not diverse enough, then the performance benefits of scaling the system to multiple processors do not scale linearly with the number of processors and, hence, propose the use of this metric for choosing the optimal minibatch size for a system. The key point to note in Eq. (1) is that the denominator contains the inner product between two gradients from *different minibatches*. Thus, orthogonal gradients would result in high gradient diversity, while similar gradients would result in low gradient diversity. The proposed framework, MuPPET, enhances this concept by considering gradients *across epochs* instead of minibatches and proposes the developed metric as a proxy for the amount of new information gained in each training step. Section 3 further expands on how the idea of gradient diversity is incorporated into the MuPPET algorithm.

3 METHODOLOGY

3.1 MULTILEVEL OPTIMISATION FOR TRAINING CNNS

Conventionally, the training process of a CNN can be expressed as in Eq. (2). Given a CNN model f parameterised with respect to a set of weights $\mathbf{w} \in \mathbb{R}^D$, where D is the number of weights of f, training involves a search for weight values that minimise the task-specific empirical loss, $Loss$, on the target dataset. Typically, a fixed arithmetic precision is employed across the training algorithm with FP32 currently being the *de facto* representation used by the deep learning community.

$$\min_{\mathbf{w}^{(\text{FP32})} \in \mathbb{R}^D} Loss(f(\mathbf{w}^{(\text{FP32})})) \tag{2}$$

The proposed method follows a different approach by introducing a multilevel optimisation scheme (Migdalas et al., 2013) that leverages the performance gains of reduced-precision arithmetic. The single optimisation problem of Eq. (2) is transformed into a series of optimisation problems with each one employing different precision for computations, but maintaining weights storage at FP32 precision. Under this scheme, an N-level formulation comprises N sequential optimisation problems to be solved, with each level corresponding to a "finer" model.

Overall, this formulation adds a hierarchical structure to the training stage, with an increasing arithmetic precision across the hierarchy of optimisation problems. Starting from the N-th problem, the inputs, weights, and activations of the CNN model f are quantised with precision q^N, which is the lowest precision in the system and represents the coarsest version of the model. Each of the N levels progressively employs higher precision until the first level is reached, which corresponds to the

original problem of Eq. (2). Formally, at the i-th level, the optimisation problem is formulated as

$$\min_{\mathbf{w}^{(q^i)} \in \mathcal{V}} Loss(f(\mathbf{w}^{(q^i)})) \quad \text{s.t. } \mathcal{V} = \left\{ \mathbf{w}^{(q^i)} \in \mathbb{R}^D : \mathrm{w}_j^{(q^i)} \in \text{represent. range}(q^i),\ \forall j \in [1, D] \right\} \tag{3}$$

The target CNN model f uses a set of weights quantised with precision q^i and hence the solution of this optimisation problem can be interpreted as an approximation to the original problem of Eq. (2). To transition from one level to the next, the result of each level of optimisation is employed as a starting point for the next level, up to the final outermost optimisation that reduces to Eq. (2).

3.2 The MuPPET Algorithm

Fig. 1 presents the process of training a CNN using the proposed algorithm. Within each epoch, MuPPET performs mixed-precision training where the weights are stored in an FP32 master copy and are quantised to the desired fixed-point precision on-the-fly prior to execution. At epoch j, the computations for the forward and backward passes (F and B blocks respectively) are performed at the current quantised precision (q^j) and the activations as well as the gradients obtained from each layer are quantised by the quantiser module before being passed on to the next layer, or stored. At the end of each epoch, the full-precision master copy of the weights is updated using a quantised gradient matrix. As discussed in Section 3.1, the quantisation level is gradually increased over the period of the training. In the proposed multilevel optimisation formulation, switching between these optimisation levels at the correct times is crucial in order not to compromise the final validation accuracy. In this respect, MuPPET introduces a precision switching policy based on an enhanced inter-epoch gradient diversity (Yin et al., 2018) metric that dictates when to switch to the next precision in order not to degrade the final resulting accuracy. Details of the switching policy are presented in Section 3.3.

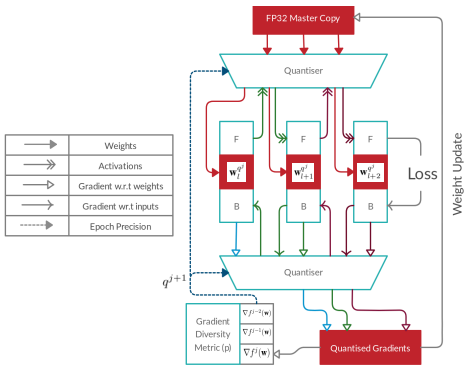

Figure 1: Precision-switching training scheme of MuPPET.

3.2.1 Quantisation Strategy

In order to implement quantised training, a quantisation strategy needs to be defined. The proposed dynamic quantisation strategy utilises block floating-point arithmetic (also known as dynamic fixed-point), where each fixed-point number is represented as a pair of an n-bit signed integer and a scale factor s, such that the value is represented as $x \times 2^{-s}$.

During the forward and backward passes of the training process, the weights and feature maps are both quantised, and the multiplication operations are performed at the same low precision. The quantisation method employs a stochastic rounding methodology (Gupta et al., 2015). The accumulation stage of the matrix-multiply operation is accumulated into a 32-bit fixed-point value to prevent overflow on the targeted networks.[1] The result of this matrix multiplication is subsequently quantised to the desired wordlength before being passed as input to the next layer. Following the block floating-point scheme, quantisation is performed such that each weight and feature map matrix in the network has a single scale factor shared by all values within the matrix. The quantisation configuration for the i-th level of optimisation and the full set of configurations are given by Eq. (4) and (5) respectively.

$$q_l^i = \left\langle \mathrm{WL}^{\text{net}}, SC_l^{\text{weights}}, SC_l^{\text{act}} \right\rangle^i, \quad \forall l \in [1, |\mathcal{L}|] \tag{4}$$

$$q^i = \left\langle q_l^i \mid \forall l \in [1, |\mathcal{L}|] \right\rangle \tag{5}$$

where $|\mathcal{L}|$ is the number of layers of the target network, WL^{net} is the fixed wordlength across the network, SC_l^{weights} and SC_l^{act} are the scaling factors for the weights and activations, respectively,

[1] The accumulator wordlength is large enough to accommodate the current CNN models, without overflow.

of the l-th layer for the i-th level of optimisation. As a result, for N levels, there are N distinct quantisation schemes; $N-1$ of these schemes are with varying fixed-point precisions, and the finest level of quantisation, q^1, is single-precision floating-point (FP32).

3.2.2 INFORMATION TRANSFER BETWEEN LEVELS

Employing multilevel training for CNNs requires an appropriate mechanism for transferring information between levels. To achieve this, the proposed optimiser maintains a master copy of the weights in full precision (FP23) throughout the optimisation levels. Similar to mixed-precision training (Micikevicius et al., 2018), at each level the SGD update step is performed by accumulating a fixed-point gradient value into the FP32 master copy of the weights. Starting from the coarsest quantisation level $i = N$, to transfer the solution from level i to level $i-1$, the master copy is quantised using the quantisation scheme q^{i-1}. With this approach, the weights are maintained in FP32 and are quantised on-the-fly during run time in order to be utilised in each training step, as $\mathbf{w}^{(q^{i-1})} \leftarrow \text{Quantise}\left(\mathbf{w}_{\text{master}}^{(\text{FP32})}, q^{i-1}\right)$.

3.3 PRECISION SWITCHING POLICY

The metric to decide when to switch between levels of quantisation is inspired by Yin et al. (2018) and based on the concept of gradient diversity (Eq. (1)). As discussed in Section 2, Yin et al. (2018) compute the gradient diversity between gradients across minibatches. Instead, MuPPET computes $\Delta_{\mathcal{S}}(\mathbf{w})$ between gradients across epochs instead of minibatches as a proxy to measure the information that is obtained during the training process; the lower the diversity between the gradients, the less information this level of quantisation is providing towards the training of the model. Therefore, the proposed method comprises a novel normalised inter-epoch version of the gradient diversity along with a run-time policy to determine the epochs to switch precision.

The following policy is employed to determine when a precision switch is to be performed. For a network with layers $\mathcal{L}$ and a quantisation scheme q^i that was switched into at epoch e:

1. For each epoch j and each layer $l \in \mathcal{L}$, the last gradient, $\nabla f_l^j(\mathbf{w})$, is stored.
2. After r (resolution) number of epochs, the inter-epoch gradient diversity at epoch j is

$$\Delta_{\mathcal{S}}(\mathbf{w})^j = \frac{\sum_{\forall l \in \mathcal{L}} \frac{\sum_{k=j-r}^{j} ||\nabla f_l^k(\mathbf{w})||_2^2}{||\sum_{k=j-r}^{j} \nabla f_l^k(\mathbf{w})||_2^2}}{|\mathcal{L}|} \tag{6}$$

3. At an epoch j, given a set of gradient diversities $\mathcal{S}(j) = \left\{\Delta_{\mathcal{S}}(\mathbf{w})^i \quad \forall \ e \leq i < j\right\}$, the ratio $p = \frac{\max \mathcal{S}(j)}{\Delta_{\mathcal{S}}(\mathbf{w})^j}$ is calculated.
4. An empirically determined decaying threshold $T = \alpha + \beta e^{-\lambda j}$ (7) is placed on the ratio p.
5. If the p violates y more than γ times, a precision switch is triggered and $\mathcal{S}(j) = \emptyset$.

3.3.1 HYPERPARAMETERS

The hyperparameters for the proposed MuPPET algorithm are the following: 1) values of α, β, and λ that define the decaying threshold from Eq. (7), 2) the number of threshold violations allowed before the precision change is triggered (γ), 3) the resolution r, 4) the set of precisions at which training is performed, and 5) the epochs at which the learning rate is changed. The values of α, β, λ, r, and γ were set at 1, 1.5, 0.1, 3, and 2 respectively after empirical cross-validation. These were tuned by running training on AlexNet and ResNet20 on the CIFAR-10 dataset. All MuPPET hyperparameters remain the same regardless of network or dataset. Regarding training hyperparameters, batch size was increased from 128 to 256 going from CIFAR-10 to ImageNet. All other training hyperparameters, mainly learning rate, weight decay and momentum, remained constant. The remaining hyperparameters such as convolutoin type, distribution approach, loss calculation, amongst others, followed framework defaults. Analysis of generalisability and the training hyperparameters used are presented in Section 5. The levels of quantised precisions at which training was performed were 8-, 12-, 14- and 16-bit fixed-point. Precisions below this did not result in any progress towards convergence for any networks.

Overall, MuPPET introduces a policy that allows to decide at run time the best point to switch between quantisation levels. After training at 16-bit fixed-point, the rest of the training is performed at FP32 until the desired validation accuracy is reached. Decaying the learning rate causes a finer exploration of the optimisation space as does increasing the quantisation level. Therefore, the learning rate was kept constant during quantised training and was decayed only after switching to FP32.

4 EVALUATION OF MUPPET

4.1 PRECISION SWITCHING

To evaluate the ability of MuPPET to effectively choose an epoch to switch precision at, AlexNet and ResNet20 were first trained using MuPPET on the CIFAR-100 dataset, and the epochs at which the learning switched occured was recorded. The hyperparameters for MuPPET were kept the same across all runs. Following this, AlexNet was trained using only 8-bit fixed-point computations updating an FP32 master copy of weights with learning rate changes performed at the same epochs as MuPPET, and the overall number of epochs identical to that run by MuPPET. This way, the only hyperparameter that differed between these runs was the precision at which computations were performed. Using checkpoints from this 8-bit training run, the precision was switched from 8-bit to FP32 at epochs 10, 15, 25, 50, and 75. The zero column remains in 8-bit fixed-point for the entire duration of training. The best validation accuracy for each of these runs is shown in Table 1. The value in brackets next to the validation accuracy of the MuPPET run is the epoch at which MuPPET switched out of 8-bit into 12-bit precision.

	Switching Epoch (8-bit to FP32)						
	0	10	15	25	50	75	**MuPPET**
AlexNet	36.6	39.0	37.8	37.9	37.6	37.3	38.0 (19)
ResNet20	64.5	64.4	65.1	65.5	65.4	65.3	65.8 (37)

Table 1: Top-1 validation accuracy (%) on CIFAR-100 switching from 8-bit fixed-point to FP32 at epochs 10, 15, 25, 50 and 75

It is seen that not switching at all causes the lowest validation accuracy, hence demonstrating that a precision switching metric is necessary when training at precisions as low as 8-bit fixed-point. With hindsight, the range of optimal switching epochs differ between AlexNet (10-15) and ResNet20 (25-50). For ResNet20, MuPPET performs as expected and switches out of 8-bit precision at epoch 37 which falls well within the range of optimal switching epochs seen from hindsight. Although for AlexNet MuPPET switches later than would be expected, in doing so it manages to exploit computational gains from reduced-precision arithmetic to a greater extent while limiting damage to the validation accuracy.

4.2 GENERALISABILITY

The MuPPET framework was also evaluated on its applicability across epochs, networks and datasets. Figure 2 shows the value of the metric p over the epochs in blue, and the decaying threshold described in Eq. (7) in orange. The number of epochs for which training in each precision was performed is shown by the various overlay colours. The graphs show that across various networks and datasets, the values of p stay relatively similar, backing the choice of a universal decaying factor. Furthermore, empirical results for CIFAR-10 indicated that changing from one fixed-point precision to another too early in the training process had a negative impact on the final validation accuracy. Using a decaying threshold ensures that the value of p needs to be much higher in the initial epochs to trigger a precision change due to the volatility of p in early epochs of training.

Generalisability across epochs is obtained as p accounts for the change in information relative to the maximum information available since the last precision change. Hence, the metric acknowledges the presence of temporal variations in information provided by the gradients. *Generalisability across networks* and *datasets* is maintained as p measures a ratio. Consequently, the absolute values of gradients which could vary between networks and datasets, matter less.

5 RESULTS

5.1 PERFORMANCE EVALUATION

The accuracy results presented in this section utilised the proposed stochastic quantisation strategy. The methodology was developed using PyTorch. As the framework does not natively support low-

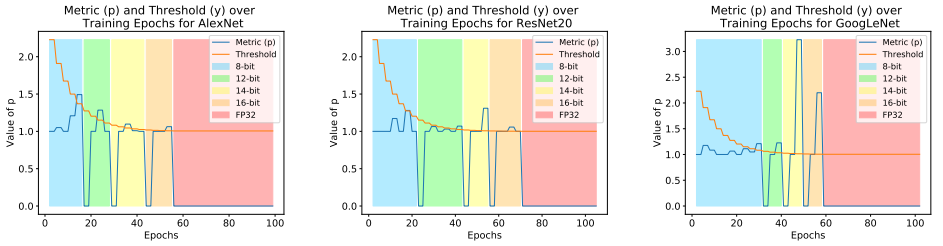

(a) AlexNet - CIFAR-10 (b) ResNet20 - CIFAR-10 (c) GoogLeNet - CIFAR-10

(d) AlexNet - ImageNet (e) ResNet18 - ImageNet (f) GoogLeNet - ImageNet

Figure 2: Demonstration of the generalisability of p over networks, datasets and epochs.

precision implementations, all quantisation and computations corresponding to 8-, 12-, 14-, and 16-bit precisions were performed through emulation on floating-point hardware. All hyperparameters not specified below were left as PyTorch defaults. For all networks, an SGD optimiser was used with batch sizes 128 on CIFAR-10 or 256 on ImageNet, momentum of 0.9 and weight decay of $1e^{-4}$.

As a baseline, an FP32 model with identical hyperparameters (except for batch size) was trained. The baseline FP32 training was performed by training for 150 epochs and reducing the learning rate by a factor of 10 at epochs 50 and 100. In order to achieve comparable final validation accuracy to the FP32 baseline, once MuPPET triggered a precision change out of 16-bit fixed-point, 45 training epochs at FP32 precision were performed. The learning rate was reduced by a factor of 10 every 15 FP32 training epochs. For AlexNet, ResNet18, ResNet20, and GoogLeNet, the initial learning rate was set to 0.01, 0.1, 0.1, and 0.001 respectively.

	CIFAR-10			**ImageNet**		
	FP32	MuPPET	Diff (pp)	FP32	MuPPET	Diff (pp)
AlexNet	75.45	74.49	-0.96	56.21	55.33	-0.88
ResNet	90.08	90.86	0.78	69.48	69.09	-0.39
GoogLeNet	89.23	89.47	0.24	59.15	63.70	4.55

Table 2: Top-1 validation accuracy (%) on CIFAR-10 and ImageNet for FP32 baseline and MuPPET

Table 2 presents the achieved Top-1 validation accuracy of the proposed method and the FP32 baseline, together with the accuracy difference in percentage points (pp). As shown on the table, MuPPET is able to provide comparable Top-1 validation accuracy to standard FP32 training across both networks and datasets. Due to a sub-optimal training setup of GoogLeNet on ImageNet, the baseline and MuPPET training severely underperformed compared to the reported state-of-the-art works. Nevertheless, the results demonstrate the quality of training with MuPPET using identical hyperparameters. As a result, MuPPET's performance demonstrates the effectiveness of the precision switching strategy in maintaining accuracy while allowing for increased performance by running many epochs at lower precision.

5.2 Wall-clock Time Improvements

This section explores the gains in estimated wall-clock time of the proposed method with respect to baseline FP32 training, Mixed Precision training by Micikevicius et al. (2018) and MuPPET's theoretical bound in acceleration that would be achieved by optimising the stochasitc rounding implementation (Table 3). For all performance results, the target platform was an NVIDIA RTX 2080

Ti GPU. At the moment, deep-learning frameworks, such as PyTorch, do not provide native support for reduced-precision hardware. Consequently, the wall-clock times provided in Table 3 were estimated using a performance model developed with NVIDIA's CUTLASS library (Kerr et al., 2018) for reduced-precision general matrix-multiplication (GEMM) employing the latest Turing architecture GPUs. The GEMMs that were accelerated were in the convolutional and fully-connected layers of each network. INT8 hardware was used to profile the 8-bit precision, while FP16 hardware was used to profile 12-, 14-, and 16-bit computations as well as Mixed Precision (Micikevicius et al., 2018) wall-clock time. CUTLASS (Kerr et al., 2018) natively implements bit-packing to capitalise on improved memory bandwidth utilisation.

As shown on Table 3, MuPPET consistently achieves 1.25-1.32× speedup over the FP32 baseline across the networks when targeting ImageNet on the given GPU. With respect to Mixed Precision by Micikevicius et al. (2018), the proposed method outperforms it on AlexNet by 1.23× and delivers comparable performance for ResNet18 and GoogLeNet. Currently, the absence of native quantisation support, and hence the necessity to emulate quantisation and the associated overheads, is the limiting factor for MuPPET to achieve higher processing speed. In this respect, with an optimised quantisation implementation, our method would yield 1.05× and 1.48× speedup for ResNet18 and GoogLeNet respectively over Mixed Precision. Additionally, performing 12-, 14- and 16-bit computations on precision-optimised fixed-point hardware would further amplify MuPPET's potential gains due to the increased parallelisation.

Similar to the analysis presented in Section 5.1, Micikevicius et al. (2018) and Wang et al. (2018) compare their respective schemes to baseline FP32 training performed by them. The reported results demonstrate that their methods achieve similar accuracy results to our method by lying close to the respective FP32 training accuracy. As Wang et al. (2018) do not provide any results in terms of gains in wall-clock times and since they use custom FP8 hardware, it could not be directly compared to our method.

	FP32 (Baseline)	**Mixed Prec (Micikevicius et al., 2018)**	**MuPPET**	**MuPPET (Theoretical Limit)**
AlexNet	30:13 (1×)	29.20 (1.03×)	23:52 (1.27×)	20:25 (1.48×)
ResNet18	132:46 (1×)	97:25 (1.36×)	100:19 (1.32×)	92:43 (1.43×)
GoogLeNet	152:28 (1×)	122:51 (1.24×)	122:13 (1.25×)	82:38 (1.84×)

Table 3: Wall-clock time (in GPU hours:minutes) and relative acceleration comparison across networks targeting ImageNet

6 CONCLUSION

This paper proposes MuPPET, a novel low-precision CNN training scheme that combines the use of fixed-point and floating-point representations to produce a network trained for FP32 inference. By introducing a precision-switching mechanism that decides at run time the best transition point between different precision regimes, the proposed framework achieves Top-1 validation accuracies comparable to that achieved by state-of-the-art FP32 training regimes while delivering significant speedup in terms of training time. Quantitative evaluation demonstrates that MuPPET's training strategy generalises across CNN architectures and datasets by adapting the training process to the target CNN-dataset pair during run time. Overall, MuPPET enables the utilisation of the low-precision hardware units available on modern, specialised processors for machine learning, such as next-generation GPUs, FPGAs and TPUs, in order to yield improvement in training time and energy efficiency without impacting the resulting accuracy.

Future work will focus on the application of the proposed framework to the training of LSTMs and RNNs, where the training process is more sensitive to the quantisation of the gradients, as well as to the extension of MuPPET to include the batch size and the learning rate as part of its hyperparameters. Exploring the mapping of MuPPET onto FPGA systems yields a greater performance per watt significantly reducing the power budget and consequently operational costs. Finally, investigating improved quantisation techniques can provide training convergence for bitwidths even lower than 8-bit fixed-point.

REFERENCES

Dan Alistarh, Demjan Grubic, Jerry Li, Ryota Tomioka, and Milan Vojnovic. QSGD: Communication-Efficient SGD via Gradient Quantization and Encoding. In *Advances in Neural Information Processing Systems 30*, pp. 1709–1720. 2017.

Han Cai, Tianyao Chen, Weinan Zhang, Yong Yu, and Jun Wang. Efficient Architecture Search by Network Transformation. In *Thirty-Second AAAI Conference on Artificial Intelligence*, 2018.

Xi Chen, Xiaolin Hu, Ningyi Xu, Hucheng Zhou, Hucheng Zhou, and Ningyi Xu. FxpNet: Training deep convolutional neural network in fixed-point representation. In *International Joint Conference on Neural Networks (IJCNN 2017)*, May 2017.

Xiaoming Chen, Danny Ziyi Chen, Yinhe Han, and Xiaobo Sharon Hu. moDNN: Memory Optimal Deep Neural Network Training on Graphics Processing Units. *IEEE Transactions on Parallel and Distributed Systems*, 30(3):646661, 2019.

Matthieu Courbariaux, Yoshua Bengio, and Jean-Pierre David. Training deep neural networks with low precision multiplications. In *Workshop in International Conference in Learning Representations*, 2015.

Christopher De Sa, Matthew Feldman, Christopher Ré, and Kunle Olukotun. Understanding and Optimizing Asynchronous Low-Precision Stochastic Gradient Descent. In *44th Annual International Symposium on Computer Architecture (ISCA)*, pp. 561–574, 2017.

Christopher M De Sa, Ce Zhang, Kunle Olukotun, Christopher Ré, and Christopher Ré. Taming the Wild: A Unified Analysis of Hogwild-Style Algorithms. In *Advances in Neural Information Processing Systems 28*, pp. 2674–2682. 2015.

Jia Deng, Wei Dong, Richard Socher, Li-Jia Li, Kai Li, and Li Fei-Fei. ImageNet: A Large-Scale Hierarchical Image Database. In *2009 IEEE Conference on Computer Vision and Pattern Recognition (CVPR)*, pp. 248–255, 2009.

Aditya Devarakonda, Maxim Naumov, and Michael Garland. AdaBatch: Adaptive Batch Sizes for Training Deep Neural Networks. *arXiv:1712.02029 [cs, stat]*, 2017.

J. Fowers, K. Ovtcharov, M. Papamichael, T. Massengill, M. Liu, D. Lo, S. Alkalay, M. Haselman, L. Adams, M. Ghandi, S. Heil, P. Patel, A. Sapek, G. Weisz, L. Woods, S. Lanka, S. K. Reinhardt, A. M. Caulfield, E. S. Chung, and D. Burger. A Configurable Cloud-Scale DNN Processor for Real-Time AI. In *2018 ACM/IEEE 45th Annual International Symposium on Computer Architecture (ISCA)*, pp. 1–14, 2018.

C. Gan, Naiyan Wang, Y. Yang, Dit-Yan Yeung, and A. G. Hauptmann. DevNet: A Deep Event Network for Multimedia Event Detection and Evidence Recounting. In *2015 IEEE Conference on Computer Vision and Pattern Recognition (CVPR)*, pp. 2568–2577, 2015.

D. Gandhi, L. Pinto, and A. Gupta. Learning to Fly by Crashing. In *2017 IEEE/RSJ International Conference on Intelligent Robots and Systems (IROS)*, pp. 3948–3955, 2017.

A Geiger, P Lenz, C Stiller, and R Urtasun. Vision meets robotics: The KITTI dataset. *The International Journal of Robotics Research*, 32(11):1231–1237, 2013.

Suyog Gupta, Ankur Agrawal, Kailash Gopalakrishnan, and Pritish Narayanan. Deep Learning with Limited Numerical Precision. In *32nd International Conference on Machine Learning (ICML)*, pp. 1737–1746, 2015.

K. He, X. Zhang, S. Ren, and J. Sun. Deep Residual Learning for Image Recognition. In *2016 IEEE Conference on Computer Vision and Pattern Recognition (CVPR)*, pp. 770–778, 2016.

K. He, G. Gkioxari, P. Dollar, and R. Girshick. Mask R-CNN. *IEEE Transactions on Pattern Analysis and Machine Intelligence (TPAMI)*, 2018.

Gao Huang, Zhuang Liu, Laurens van der Maaten, and Kilian Q Weinberger. Densely Connected Convolutional Networks. In *2017 IEEE Conference on Computer Vision and Pattern Recognition (CVPR)*, pp. 2261–2269, 2017.

Tyler B Johnson and Carlos Guestrin. Training Deep Models Faster with Robust, Approximate Importance Sampling. In *Advances in Neural Information Processing Systems 31*, pp. 7265–7275. 2018.

Norman P. Jouppi et al. In-Datacenter Performance Analysis of a Tensor Processing Unit. In *44th Annual International Symposium on Computer Architecture (ISCA)*, pp. 1–12, 2017.

A. Karpathy, G. Toderici, S. Shetty, T. Leung, R. Sukthankar, and L. Fei-Fei. Large-Scale Video Classification with Convolutional Neural Networks. In *2014 IEEE Conference on Computer Vision and Pattern Recognition (CVPR)*, pp. 1725–1732, 2014.

Angelos Katharopoulos and Francois Fleuret. Not All Samples Are Created Equal: Deep Learning with Importance Sampling. In *Proceedings of the 35th International Conference on Machine Learning (ICML)*, volume 80, pp. 2525–2534, 2018.

Andrew Kerr, Duane Merril, Julien Demouth, and John Tran. CUTLASS: Fast Linear Algebra in CUDA C, Sep 2018. URL `https://devblogs.nvidia.com/cutlass-linear-algebra-cuda/`.

A. Kouris and C. Bouganis. Learning to Fly by MySelf: A Self-Supervised CNN-Based Approach for Autonomous Navigation. In *2018 IEEE/RSJ International Conference on Intelligent Robots and Systems (IROS)*, pp. 1–9, 2018.

Tsung-Yi Lin, Michael Maire, Serge Belongie, James Hays, Pietro Perona, Deva Ramanan, Piotr Dollár, and C. Lawrence Zitnick. Microsoft COCO: Common Objects in Context. In *European Conference on Computer Vision (ECCV)*, pp. 740–755, 2014.

Antonio Loquercio, Ana I. Maqueda, Carlos R. del Blanco, and Davide Scaramuzza. DroNet: Learning to Fly by Driving. *IEEE Robotics and Automation Letters*, 3(2):1088–1095, 2018.

Ilya Loshchilov and Frank Hutter. Online Batch Selection for Faster Training of Neural Networks. In *Workshop at International Conference on Learning Representations*, 2016.

Paulius Micikevicius, Sharan Narang, Jonah Alben, Gregory Diamos, Erich Elsen, David Garcia, Boris Ginsburg, Michael Houston, Oleksii Kuchaiev, Ganesh Venkatesh, and Hao Wu. Mixed Precision Training. In *International Conference on Learning Representations (ICLR)*, 2018.

Athanasios Migdalas, Panos M Pardalos, and Peter Värbrand. *Multilevel Optimization: Algorithms and Applications*, volume 20. Springer Science & Business Media, 2013.

Joe Yue-Hei Ng, M. Hausknecht, S. Vijayanarasimhan, O. Vinyals, R. Monga, and G. Toderici. Beyond Short Snippets: Deep Networks for Video Classification. In *2015 IEEE Conference on Computer Vision and Pattern Recognition (CVPR)*, pp. 4694–4702, 2015.

Xinyu Peng, Li Li, and Fei-Yue Wang. Accelerating Minibatch Stochastic Gradient Descent using Typicality Sampling. *arXiv:1903.04192 [cs, math, stat]*, 2019.

Minsoo Rhu, Natalia Gimelshein, Jason Clemons, Arslan Zulfiqar, and Stephen W. Keckler. vDNN: Virtualized Deep Neural Networks for Scalable, Memory-efficient Neural Network Design. In *The 49th Annual IEEE/ACM International Symposium on Microarchitecture (MICRO)*, pp. 18:1–18:13, 2016.

Karen Simonyan and Andrew Zisserman. Two-Stream Convolutional Networks for Action Recognition in Videos. In *Advances in Neural Information Processing Systems 27*, pp. 568–576. 2014.

V. Sze, Y. Chen, T. Yang, and J. S. Emer. Efficient Processing of Deep Neural Networks: A Tutorial and Survey. *Proceedings of the IEEE*, 105(12):2295–2329, 2017.

Christian Szegedy, Sergey Ioffe, Vincent Vanhoucke, and Alexander Alemi. Inception-v4, Inception-ResNet and the Impact of Residual Connections on Learning. In *AAAI Conference on Artificial Intelligence*, 2017.

G. Varol, I. Laptev, and C. Schmid. Long-Term Temporal Convolutions for Action Recognition. *IEEE Transactions on Pattern Analysis and Machine Intelligence (TPAMI)*, 40(6):1510–1517, 2018.

Naigang Wang, Jungwook Choi, Daniel Brand, Chia-Yu Chen, and Kailash Gopalakrishnan. Training Deep Neural Networks with 8-bit Floating Point Numbers. In *Advances in Neural Information Processing Systems 31*, pp. 7675–7684. 2018.

Dong Yin, Ashwin Pananjady, Max Lam, Dimitris Papailiopoulos, Kannan Ramchandran, and Peter Bartlett. Gradient Diversity: a Key Ingredient for Scalable Distributed Learning. In *21st International Conference on Artificial Intelligence and Statistics (AISTATS)*, pp. 1998–2007, 2018.

Z. Zhong, J. Yan, W. Wu, J. Shao, and C. Liu. Practical Block-Wise Neural Network Architecture Generation. In *2018 IEEE/CVF Conference on Computer Vision and Pattern Recognition (CVPR)*, pp. 2423–2432, 2018.

Shuchang Zhou, Zekun Ni, Xinyu Zhou, He Wen, Yuxin Wu, and Yuheng Zou. DoReFa-Net: Training Low Bitwidth Convolutional Neural Networks with Low Bitwidth Gradients. *CoRR*, 2016.